JOURNAL OF PROPULSION AND POWER
Vol. 12, No. 6, November–December 1996

# Low-Power Ammonia Arcjet: Numerical Simulations and Laser-Induced Fluorescence Measurements

David Burtner* and Dennis Keefer†
*University of Tennessee Space Institute, Tullahoma, Tennessee 37388*
and
Wim Ruyten‡
*Sverdrup Technology, Inc., Arnold Air Force Base, Tennessee 37389*

**Numerical simulations were performed for a 1-kW ammonia arcjet using the University of Tennessee Space Institute equilibrium arcjet computational code. Thrust predicted by the code was compared with experimental data obtained from a thrust stand, and calculations of exit plane flow conditions were compared with data obtained from multiplexed laser induced fluorescence (LIF) experiments. The code predictions for thrust follow the same trends as the experimentally measured values, but they significantly overpredict the absolute values. Multiplexed LIF experiments were performed using both atomic nitrogen and atomic hydrogen in the plume. When nitrogen is used the effects of scattering can be significantly reduced by spectral discrimination of the fluorescence. The experiments reveal that the two species have different velocities at a position 1 mm downstream from the nozzle exit plane. The code predictions of the velocity at the exit plane have been compared with the LIF experiments. These comparisons were not conclusive because the propellant velocity can change significantly between the exit plane, where the code predictions are made, and 1 mm downstream, where the LIF measurements are made. The discrepancy between these code predictions and the experimental results highlight the inadequacy of equilibrium computational codes to accurately simulate arcjet flows.**

## Introduction

An effort has been underway at the University of Tennessee Space Institute (UTSI) since 1989 to develop a better understanding of arcjet physics using computational simulations and optical diagnostics. One version of the UTSI computational code, which assumes that the plasma flow is in thermodynamic equilibrium, was used to simulate the flow in a 1-kW arcjet operated with a simulated ammonia propellant. The predictions from this code simulation were compared with thrust stand measurements made at NASA Lewis Research Center (LeRC). The code predictions were also compared with multiplexed laser induced fluorescence (LIF) measurements made in the UTSI large vacuum facility using both hydrogen and nitrogen atomic species present in the exhaust plume.

The UTSI computational code was originally developed to simulate a laser-sustained plasma thruster.[1] A steady-state, Navier–Stokes code based on the SIMPLE algorithm of Gosman and Pun,[2] as modified by Rhie[3] to handle subsonic and supersonic flows, was extended to include radiation transfer and heat addition.[4] The code proved successful at predicting the behavior of laser-sustained plasmas[1] and radio-frequency inductive arcs,[5] and was therefore chosen as a basis for further development to permit arcjet simulations.

The original code assumed that the plasma was in local thermodynamic equilibrium (LTE), which proved reasonable for the laser-sustained plasmas that are typically operated at pressures of one to several atmospheres pressure. Initial comparisons of the UTSI arcjet code with experiments performed at LeRC[6] using a 10-kW hydrogen arcjet showed that the code overestimated performance, but predicted correct trends with propellant flow rate and power. Subsequent comparisons of the code with the experimental performance of similar water- and radiation-cooled hydrogen arcjets revealed the limitations of the LTE assumption.[7] The code has been extended to use equilibrium ammonia as a propellant and used to simulate a 1-kW ammonia arcjet. These simulations are compared with experimental thrust measurements and LIF measurements of velocity and temperature made using the NASA 1-kW arcjet operated with a simulated ammonia propellant.

The velocity distribution function of an absorbing atom can be sampled with a high degree of precision with single photon fluorescence methods using narrow-line tunable dye lasers.[8] For propellants of interest in arcjets, the only candidates for this technique are excited state atoms, since the resonance absorption lines of the atoms are all in the vacuum ultraviolet portion of the spectrum. However, the LIF technique recently has been extended to ground state hydrogen using two-photon excitation.[9] The one photon LIF technique was first demonstrated in an arcjet plume using the Balmer-alpha transition in hydrogen.[10] A multiplexed LIF method was developed at UTSI that is capable of measuring two (or more) components of velocity simultaneously. This method was first demonstrated using a 300-W arcjet operating with argon propellant.[11] This LIF technique has now been extended to use both the H-alpha and atomic nitrogen transitions to measure the exhaust plume velocity in a 1-kW arcjet using ammonia- and hydrazine-analog mixtures of hydrogen and nitrogen propellants.

## Arcjet Model

The numerical model used in this work has been described fully in past papers.[12–15] The general form of the arcjet model is a Navier–Stokes solver based on the semi-implicit pressure linked equation (SIMPLE) algorithm of Gosman and Pun,[2]

Received Nov. 2, 1994; revision received Feb. 15, 1996; accepted for publication Aug. 17, 1996. 

*Graduate Research Assistant, Center for Laser Applications. Student Member AIAA.

†B. H. Goethert Professor of Engineering Sciences and Mechanics, Center for Laser Applications. Senior Member AIAA.

‡Senior Research Engineer. Member AIAA.

which was modified by Rhie[3] to handle subsonic and supersonic flows. The capabilities for electrical or optical energy addition and radiation heat transfer were later added by Jeng and Keefer.[4]

The model uses the fluid equations for steady, axially symmetric, compressible flow. Local thermodynamic and chemical equilibrium is assumed everywhere. This assumption implies that heavy particle and electron temperatures are equal, and that all thermodynamic and transport properties, including species concentrations, can be defined by two state variables.[13] The flow is assumed to be laminar. The electromagnetic equations are also steady in time and are axially symmetric. In the absence of external fields, the axial and radial components of the magnetic field are assumed to be zero.[12]

The code solves for eight dependent variables from eight coupled partial differential equations. The dependent variables are axial velocity $u$, radial velocity $v$, azimuthal velocity $w$, static enthalpy $h$, pressure $p$, the azimuthal component of magnetic field $B_\theta$, and the axial and radial current densities $J_x$ and $J_r$, respectively. The electromagnetic equations are coupled to the fluid equations through ohmic heating and Lorentz body forces. The velocity components are obtained from conservation of momentum in three directions. The static enthalpy is obtained from the energy equation. Pressure is obtained from conservation of mass. The azimuthal component of magnetic field is described by an equation derived from Maxwell's equations and Ohm's law. The current densities are obtained from numerical derivatives of $B_\theta$.[12]

The governing equations are solved in a transformed coordinate system, which is a mapping of the true nonorthogonal and nonuniform grid to a grid of unit squares. The equation for magnetic field is linear and can be solved by direct matrix inversion. The fluid equations for $u$, $v$, $w$, $h$, and $p$ are solved sequentially using updated values of the dependent variables when they are available and the old values when updated ones have not yet been calculated. Nonlinear terms are linearized by including them in source terms.[13] As the new values of the dependent variables are calculated, they are relaxed into the previous solution. Solution iterations continue until the residual errors of the equations have been reduced to reasonably small values.[12] Upwind differencing for convective terms and fourth-order pressure smoothing maintain stability of the dependent variables during the relaxation to a final solution.[13]

A no-slip velocity boundary condition is in effect at all walls. The wall temperatures are specified at each axial location, and the normal pressure gradient on the walls is zero. The values of $v$ and $w$ and the radial derivatives of $u$, $h$, and $p$ are set to zero along the symmetry line at the center of the flow. The axial derivatives of all dependent variables are set to zero at the nozzle exit. Velocity and enthalpy are specified at the inlet based on the mass flow, inlet temperature, and inlet swirl angle, which are input parameters to the program.[13]

The thermodynamic and transport properties for ammonia are stored in lookup tables that the program can access during operation. Temperature is stored as a function of static enthalpy for a range of pressures. The transport properties viscosity $\mu$, thermal conductivity $k$, and electrical conductivity $s$ are stored as functions of temperature and pressure.[13] The property table calculations were made assuming a nonideal plasma in LTE. A nonideal plasma occurs when the electrons have kinetic energies on the order of the Coulomb potential, so that only a few electrons inhabit a Debye sphere.[16]

## Experiments

### Thrust Stand Measurements

Thrust stand measurements were performed at the LeRC so that thrust calculated by the code could be compared to experimental data. The thrust stand used for these measurements was the NASA inverted pendulum design.[17,18] Displacement is measured with a linear variable differential transformer. Oscillations are removed by actively damping the system with an electric forcing coil. To prevent thermal drift, active cooling is used to insulate the thrust stand from heat produced by the arcjet. Water cooling lines surround the arcjet support column so that heat cannot conduct to the flexures. The entire apparatus is shielded from arcjet radiation by surrounding the stand in a water-cooled metal enclosure. The propellant enters the arcjet from a line that travels through the thrust stand assembly. Electric power is supplied to the arcjet from two insulated wires that hang down from the inside of the vacuum chamber.[18]

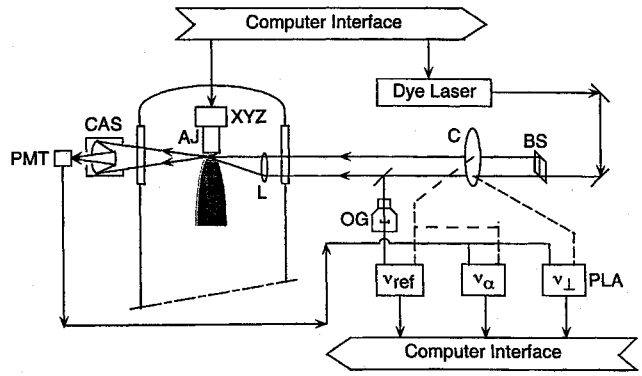


**Fig. 1 Schematic of the experimental setup. CAS is the Cassegrain telescope, PMT is the photomultiplier detector, XYZ is the translation stage that moves the arcjet, AJ is the arcjet, L is the lens, OG is the optogalvanic cell, C is a two-frequency chopper, and BS is a beamsplitter prism. The three phase-locked amplifiers (PLA) provide the reference signal $\nu_{ref}$, the angled beam signal $\nu_\alpha$, and the perpendicular beam signal $\nu_\perp$.**

The thrust stand was calibrated before taking arcjet thrust data. The slope and zero of the thrust vs displacement curve are measured with the arcjet fully installed in the evacuated chamber, so that any nonlinear effects of the propellant tubes, electric wires, and gravity will be taken into account. The calibration is accomplished by remotely loading the flexures with several 4-g weights.[18]

### LIF Measurements

LIF has been used at UTSI to measure velocity and temperature in argon and ammonia arcjet plumes.[11,19] The principle of the LIF technique is to use a tunable, narrow-band laser to excite an atomic transition in one of the species in the plume. Absorption of the laser is indicated when fluorescence radiation is detected. The amount of absorption detected as a function of laser frequency provides a measurement of the Doppler profile of the fluorescing atom. The mean velocity and temperature of the plume can then be determined by analyzing the Doppler profile.[15]

A schematic of the LIF experiment is shown in Fig. 1. The experiments were conducted in the large (3 m diam by 6 m long) UTSI vacuum chamber. For the arcjet experiments the cryopumps were not used, and the chamber was pumped with mechanical pumps with 480-cfm capacity. A portion of the laser beam is directed into a hollow cathode lamp to provide a stationary reference signal produced by the optogalvanic effect from the same atomic transition that is used for the plume measurements.[20] The remaining laser beam is split into two beams that are focused onto a point in the arcjet plume. One beam intersects the plume perpendicular to the arcjet axis, and the other intersects at an angle of approximately 70 deg to the arcjet axis.

In earlier experiments using argon propellant, the LIF signal was detected with a lens and photodiode mounted inside the vacuum chamber.[11] However, the LIF signals from hydrogen and nitrogen are weaker than the signal from argon, and a more sensitive method of detection was required. For this experiment, the fluorescence was collected by imaging the beam intersection point onto a photomultiplier tube using a Cassegrain

telescope and a small aperture mounted outside the test chamber. The external aperture limited the spatial resolution in the direction of the beams to slightly less than 1 mm. Phase-locked detection, using a dual-frequency chopper and lock-in amplifiers, separates the multiplexed LIF signal into distinct signals from each of the two laser beams. From these two signals, the radial and axial plume velocity components can be determined simultaneously.

The initial LIF experiments utilized the Balmer-alpha transition of atomic hydrogen. This is the electronic transition between the second and third electronic energy levels at a wavelength of 656.28 nm.[9] The experiments were later repeated under the same arcjet conditions, but the transition between the $3s^4P$ and the $3p^4S^0$ electronic energy levels in atomic nitrogen was excited. The wavelength of this transition is 746.83 nm. Scattered light from the laser beam interactions with the arcjet and test chamber reduce the sensitivity of the measurements made with hydrogen, since both the fluorescent signal and the scattered signal from the laser have the same wavelength. This effect is particularly significant when the probe laser passes very near the arcjet nozzle. When nitrogen is used for the LIF measurement fluorescence is emitted at several wavelengths in addition to the exciting wavelength. The effect of this laser scattering was significantly reduced in the nitrogen measurements by exciting the transition at a wavelength of 746.83 nm and using a 1.2-m monochrometer to discriminate against scattered radiation and detect the fluorescence at a wavelength of 744.23 nm.

## Results and Discussion

### Comparison of Thrust Data

To evaluate the accuracy of the UTSI computer model, thrust experiments were performed for a range of electrical power inputs and propellant flows. During the thrust experiments, the background pressure in the vacuum chamber was approximately $5 \times 10^{-4}$ torr. The computer code was used to calculate the thrust for the same arcjet geometry using identical power inputs and propellant flows.

Figure 2 shows the changes in thrust when electrical power is varied and the mass flow is held constant at 37.9 mg/s. Figure 3 shows a similar comparison, but the mass flow is varied and the current supplied to the arcjet is held constant at 9.0 A. In both comparisons, the computer model significantly overpredicts the experimental values (between 24–35%), but the thrust calculated by the model follows the experimental trends with respect to power and mass flow. This suggests that the basic arcjet model is sound, but significant energy losses have been neglected. The assumption of thermal and chemical equilibrium neglects important loss mechanisms. The equilibrium model allows dissociation and ionization energies to be recovered in the nozzle expansion section that normally would be lost because of frozen flow conditions. The equilibrium model also does not account for heat conduction to the wall from the diffusion of high-energy electrons from the high-temperature core through the cold boundary layer. The assumption of equilibrium also alters the character of the flow by changing the electrical conductivity, which controls the spatial distribution of power absorption in the flow.

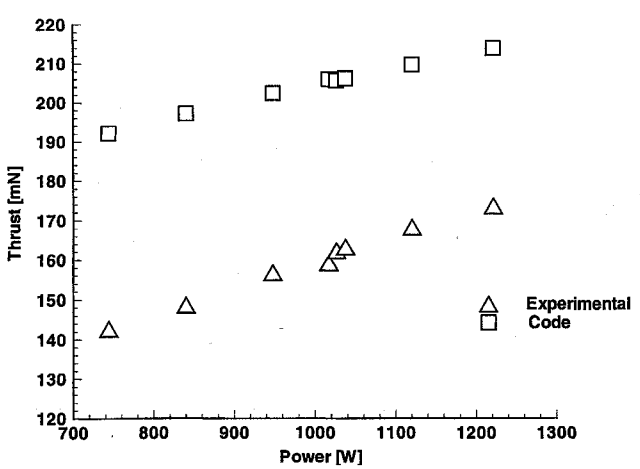


**Fig. 2 Comparison of measured and computed thrust: thrust vs power at constant mass flow.**

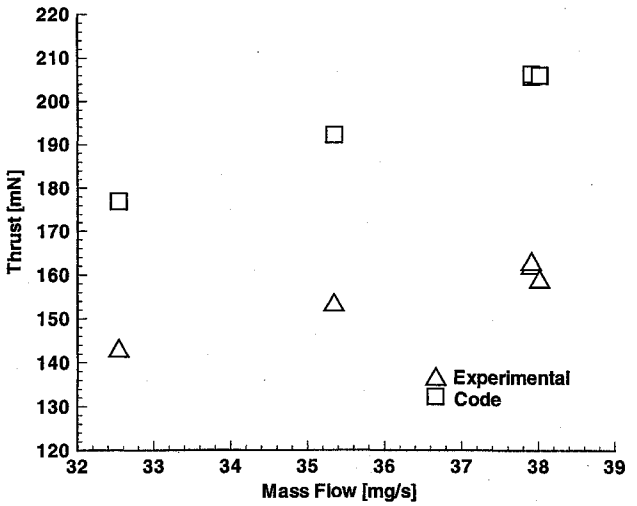


**Fig. 3 Comparison of measured and computed thrust: thrust vs mass flow at constant current.**

### Comparison of Velocity and Temperature Data

The multiplexed LIF technique was used to measure the plume velocities and temperatures in radial scans across the exit plane. One radial scan was performed by probing atomic hydrogen in the flow and another scan was performed probing atomic nitrogen. The LIF experiments were performed with the arcjet running at a current of 9.0 A and an electrical power input of 999 W with a mass flow of 37.9 mg/s. All LIF measurements were taken approximately 1-mm downstream from the nozzle exit plane. During the experiments, the ambient pressure in the vacuum chamber was approximately 1 torr, which is much higher than the background pressure of the thrust stand experiments.

The arcjet flow at the nozzle exit is underexpanded, meaning that the pressure at the exit plane is much higher than the ambient pressure. At 1 mm downstream from the exit plane, radial expansion at the nozzle lip and boundary-layer mixing with the relatively high-pressure ambient gas in the test chamber cause the flowfield properties to be distorted at the outer edges. The calculations of the model are made at the nozzle exit plane, so that valid comparisons can only be made near the center of the flow.

Figures 4 and 5 compare measured radial and axial velocity components obtained using both hydrogen and nitrogen lines to the velocities calculated by the model. Near the center of the flow the measured axial component of the nitrogen velocity is approximately 1000 m/s greater than the code predictions, whereas the axial component of the hydrogen velocity is approximately 500 m/s greater than the code predictions. The theoretical accuracy of the velocity measurements based on the width of the laser line is only a few m/s, but the achieved accuracy depends on the stability of the laser and the flow velocity during the frequency scan. The achieved accuracy for these experiments is estimated to be approximately $\pm 30$ m/s. The repeatability of the measurements can be estimated from the multiple data points shown for hydrogen in Fig. 5, which were obtained with the same experimental setup on two successive days. The difference in the velocities measured at 1.0, 1.5, and 2.5 mm is approximately 100 m/s. An interesting result of the experiments is that atomic hydrogen and nitrogen

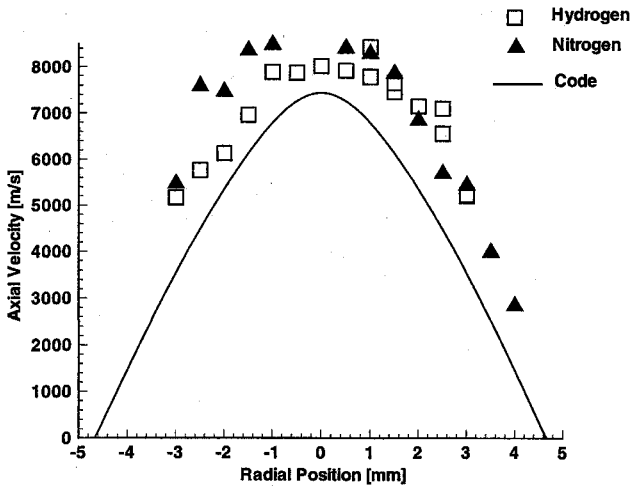


**Fig. 4 Comparison of measured and computed axial velocities at the nozzle exit.**

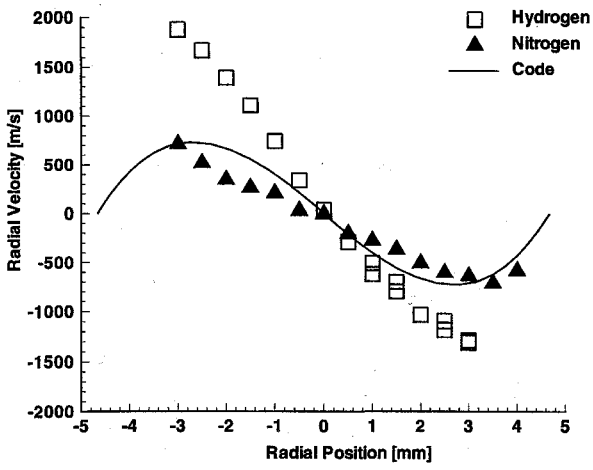


**Fig. 5 Comparison of measured and computed radial velocities at the nozzle exit.**

in the flow have different velocities. The radial expansion of hydrogen is much faster than the nitrogen, but the nitrogen has a slightly larger axial component of velocity. Separation of hydrogen and nitrogen also has been observed with mass spectrometer experiments in a hydrazine arcjet by Welle et al.[21]

From the thrust measurements it was seen that the UTSI arcjet code overpredicted the thrust by at least 24%. Therefore, the code would also be expected to overpredict the axial velocity. However, the axial velocities calculated by the code are significantly less than the measured values. It does not seem logical that the model could simultaneously overpredict thrust and underpredict axial velocity.

One possible explanation for this discrepancy is that the code may incorrectly calculate the distribution of propellant mass at the exit plane. Thrust can be calculated by integrating the momentum of the flow at the exit plane. If the model calculations of the density profile at the exit plane are sufficiently different from the actual flow, it would be possible for the calculation of thrust to be higher than the experimental value, even though the computed velocities at the exit plane are lower than experimental values. For example, if the code overestimates the density in the center of the flow, the contribution to the momentum integral would be large where the velocity is large, and the contribution would be small at the edge where the velocity is small. If the calculated density is sufficiently concentrated in the center of the flow, the calculated thrust will be larger than the value obtained from the thrust stand experiment, even though the computed axial velocity is smaller everywhere than the experimental axial velocity.

Another possible explanation for the disagreement between axial velocity and thrust has to do with the differences in the locations of the code predictions and the experimental measurements. The LIF measurements are made 1 mm downstream from the nozzle exit, but the code calculations are made exactly at the exit plane. The underexpanded flow will continue to accelerate axially after it leaves the nozzle. Axial acceleration of propellant downstream of the nozzle exit in an ammonia arcjet plume has been previously reported by Ruyten et al.[19,22] Since the flow is underexpanded, the supersonic expansion continues for several millimeters downstream until the flow is readjusted to the ambient pressure by the normal shock at the Mach disk.

The code prediction for radial velocity is even more difficult to evaluate. Radial expansion of the plume at the nozzle edge makes comparisons of radial velocities at the exit plane with radial velocities 1 mm downstream inappropriate. The large separation of the hydrogen and nitrogen radial velocities also make any comparisons difficult because the code assumes a continuum flow. Since any other species in the flow, such as $H_2$, $N_2$, or NH could also have different radial velocities, and the density of each of the species is unknown, the experiment cannot provide even an accurate averaged radial velocity to compare with the code predictions.

In general, the temperatures measured with LIF are less accurate than the velocity measurements for several reasons. Temperature of the plume is determined from the Gaussian width of the LIF measured Doppler profile. However, it is generally more difficult to determine accurate widths than accurate profile centers from the experimental data. The width of the profile obtained from curve fitting is sensitive to changes in amplitude and baseline offset of the LIF signal, whereas the determination of the center of the profile is relatively straightforward. As a result, temperatures determined by LIF measurements are always somewhat less reliable than the velocities.

However, there are aspects to this specific experiment that introduce additional errors to the temperature data obtained by LIF. Accurate temperature data cannot be obtained by probing the atomic hydrogen because the hydrogen Doppler profile is much wider than the limited-frequency scanning range (30-GHz) of the dye laser that was available for these experiments. An example of a measured hydrogen Doppler profile is shown in Fig. 6. It is difficult to make an accurate estimation of the width of the profile without observing the wings of the line profile where the signal goes to zero. The hydrogen Doppler profile is wide, because, at a given temperature, particles with

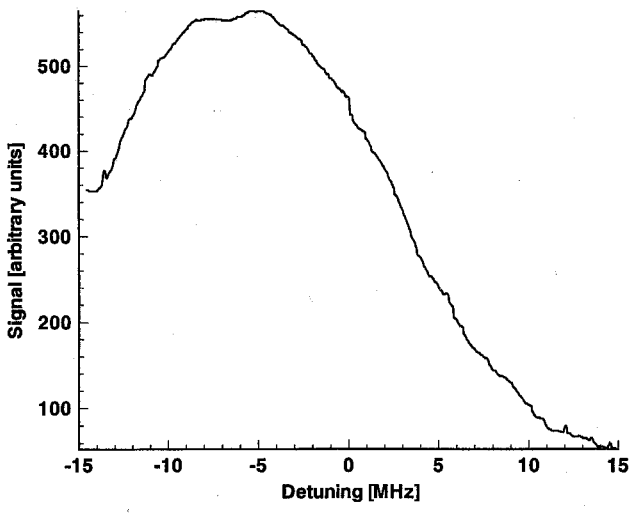


**Fig. 6 Doppler profile of atomic hydrogen showing extreme width.**

low mass have larger thermal velocities than heavier particles. The profile also appears broad because the Balmer-alpha transition consists of five overlapping fine-structure transitions.[9] Recent direct emission measurements of the hydrogen Balmer-alpha line in an arcjet indicate that Stark broadening must also be taken into account.[23] The nitrogen line profiles are narrower because of their larger mass and much smaller Stark broadening, and do not present the same difficulties for the measurement of temperature.

A radial scan of temperatures determined by probing atomic nitrogen is shown in Fig. 7. The data acquired from both the angled beam and the perpendicular beam are shown. An effect of the experimental layout introduced some additional uncertainty into the nitrogen temperature data obtained from the angled beam. After passing through the fluorescence collection volume, the angled laser beam intersected the inside of the nozzle wall essentially normal to the surface. The beam was reflected and passed back through the collection volume creating a second, shifted, and weaker Doppler profile. An example is shown in Fig. 8. When the width of the line was comparable to the Doppler shift, the second profile partially overlapped the primary profile, leading to inaccuracies in the determination of the Doppler width as shown in Fig. 9. The overlap became more pronounced at positive radial locations where the backscattered signal was stronger.

An interesting experimental result is that the temperatures acquired from the angled beam are consistently higher than the

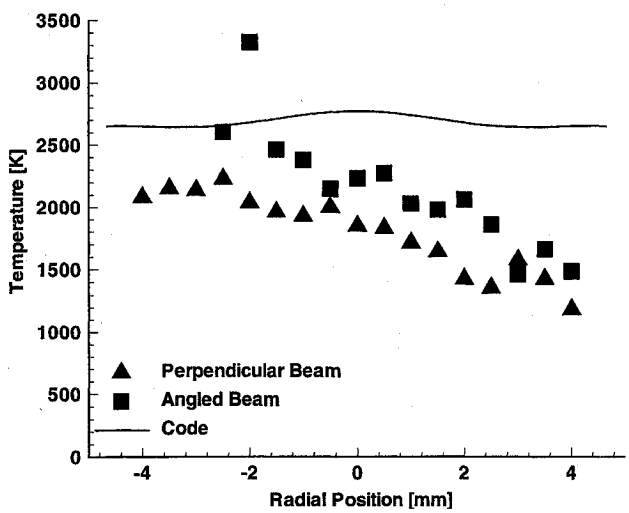


**Fig. 7 Computed temperatures compared to experimental temperatures of atomic nitrogen.**

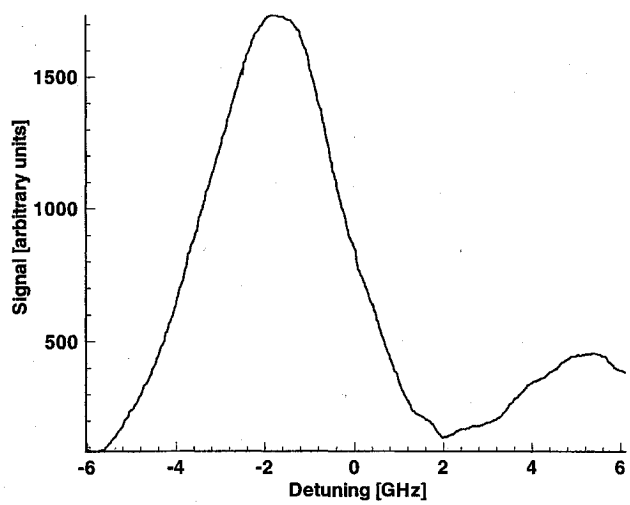


**Fig. 8 Doppler profile of atomic nitrogen showing false signal.**

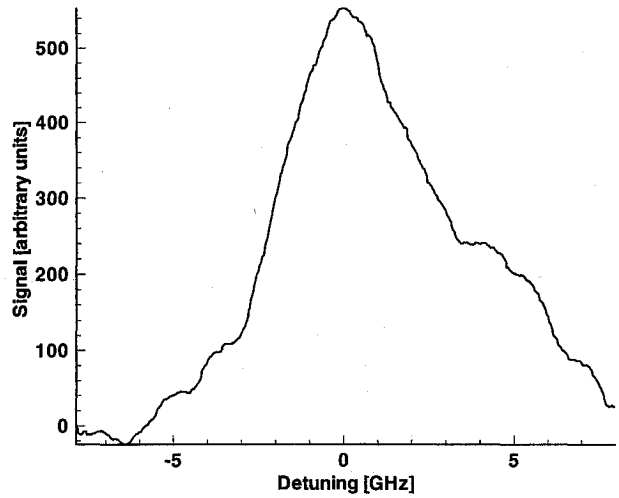


**Fig. 9 Doppler profile of atomic nitrogen showing interference from false signal.**

temperatures acquired from the perpendicular beam. There are two possible causes for the difference. One possible cause is that the velocity of the plume may be fluctuating in time as suggested by Ruyten and Keefer.[11] Changes in the velocity during the time required for the wavelength scan effectively blur the profile, causing it to broaden. Since the angled beam is affected by the large axial component of velocity, it will experience larger velocity changes and be broadened more than the perpendicular beam.

Because of the finite size of the fluorescence collection volume, the Doppler profile can also be broadened by spatial velocity gradients. The fluorescence signal is integrated over the sample volume and contains contributions from all velocities within the volume. When there is a velocity gradient in the flow, the mean velocity changes over the extent of the sample volume and superposition of the different Doppler shifts leads to a broadening of the measured signal. Near the exit plane of an arcjet, strong velocity gradients are created by the continued axial acceleration of the propellant after it leaves the nozzle. The perpendicular beam is directed perpendicular to the axis and the axial extent of the sample volume is limited to the laser beam diameter. However, the angled beam extends over a larger axial range and the broadening effect of the axial velocity gradient will be larger. Therefore, the Doppler profile detected by the angled beam will be broadened more by the effects of velocity gradients than that for the perpendicular beam.

Figure 7 shows that the temperatures calculated by the code are consistently larger than the experimental values. The temperatures predicted by the code are expected to be larger than the experiment because of the assumption of local chemical and thermodynamic equilibrium used in the code. The equilibrium assumption means that energy deposited in the internal modes of the atoms and molecules can be recovered as thermal energy, but, in reality, some of the energy leaves the nozzle while frozen in the internal energy modes and is not recovered as translational temperature.

An additional degree of uncertainty in the comparison of computed and experimental temperature is introduced because the experiment takes place 1 mm downstream from the model exit plane calculations. The continuing supersonic expansion of the propellant downstream of the exit plane I causes the temperature to decrease below its value at the exit plane.

## Conclusions

The multiplexed LIF technique for the measurement of arcjet velocity and temperature has been extended to utilize nitrogen as the sample atom. The use of nitrogen results in narrower Doppler profiles compared with hydrogen and leads

to a more accurate determination of the Doppler shift and width. Another important advantage of nitrogen is that it allows fluorescence detection at a wavelength different than the laser wavelength used to excite the fluorescence transition. This permits a monochrometer to be used to discriminate against scattered radiation from the laser beam, and measurements can, therefore, be taken closer to scattering surfaces.

Comparisons between velocities and temperatures calculated at the nozzle exit plane and LIF measurements taken 1 mm downstream were inconclusive because of the continued expansion of the flow past the exit plane. It is unknown how much the velocity and temperature differences result from inaccuracies in the model and how much they result from expansion downstream of the nozzle exit. The velocity and temperature of the propellant can change significantly in the 1-mm distance between the model exit plane calculations and the LIF radial scan. Significant differences between the measured velocities of hydrogen and nitrogen were observed, and the difference was particularly evident in the radial component of velocity. Meaningful comparisons between code predictions and LIF measurements will require that the expansion calculations be continued beyond the nozzle exit plane, or experimental measurements will have to be taken within the nozzle.

The UTSI equilibrium ammonia arcjet code correctly predicts trends in thrust with respect to power and mass flow, but does not make accurate quantitative predictions. Nonequilibrium effects are significant in the arcjet flowfield. The present equilibrium model is inadequate for arcjet simulation because it does not correctly account for frozen flow losses in the nozzle, and it does not accurately calculate electrical conductivity and power absorption.

Other comparisons between equilibrium code predictions and experimental measurements have also shown the inadequacy of the equilibrium assumptions. In particular, the UTSI equilibrium code failed to predict the large performance difference between radiation-cooled and water-cooled arcjets of similar configuration and operating parameters.[7] The UTSI arcjet code using hydrogen as a propellant has been modified to include finite rate chemistry and a two-temperature model for the plasma.[15] This new code produced significantly better performance predictions than the equilibrium code. It was found that radial diffusion of electrons and finite rate recombination had a large effect on the electron number density distributions in the constrictor and anode regions. This, in turn, made significant differences in the electrical conductivity and power input distribution, particularly in the regions near the wall of the anode. As a result of these studies, we conclude that any useful arcjet computational code must include finite rate chemistry and a two-temperature nonequilibrium plasma model to accurately simulate the arcjet. A successful arcjet code for ammonia or hydrazine will also require a set of kinetic reactions and reaction rates for the nitrogen–hydrogen system in order to accurately account for the frozen flow losses in the nozzle.

## Acknowledgments

This work was supported by a grant from the U.S. Air Force Office of Scientific Research. We gratefully acknowledge the loan of the arcjet system from the NASA Lewis Research Center. We would particularly like to thank John Sankovic and his colleagues at the NASA Lewis Research Center for their time, effort, and facilities, which allowed the thrust stand data to be collected. We are also appreciative of the work of Bob Rhodes with the computational model and the laboratory support of Newt Wright. The nonideal plasma transport properties for ammonia were calculated for us by Robert Zollweg.

## References

[1]Jeng, S.-M., Keefer, D., Welle, R., and Peters, C. E., "Laser Sustained Plasmas in Forced Convective Argon Flow, Part II: Comparison of Numerical Model with Experiment," *AIAA Journal*, Vol. 25, No. 9, 1987, pp. 1224–1230.

[2]Gosman, A. D., and Pun, W. M., "Calculation of Recirculating Flows," Imperial College, Dept. of Mechanical Engineering, Rept. HTS/74/12, London, 1974.

[3]Rhie, C. M., "A Pressure Based Navier-Stokes Solver," AIAA Paper 86-0207, Jan. 1986.

[4]Jeng, S.-M., and Keefer, D., "Theoretical Evaluation of Laser-Sustained Plasma Thruster Performance," *Journal of Propulsion and Power*, Vol. 5, No. 5, 1989, pp. 577–581.

[5]Rhodes, R. P., and Keefer, D. "Numerical Modeling of a Radio Frequency Plasma in Argon," *AIAA Journal*, Vol. 27, No. 12, 1989, pp. 1779–1784.

[6]Haag, T., and Curran, F., "High Powered Hydrogen Arcjet Performance," AIAA Paper 91-2227, June 1991.

[7]Moeller, T. M., Keefer, D., and Rhodes, R. P., "Comparison of Experimental and Numerical Results for Radiation Cooled and Water Cooled Hydrogen Arcjets," 23rd International Electric Propulsion Conf., Seattle, WA, Sept. 1993 (Paper 93-214).

[8]Demtroder, W., *Laser Spectroscopy*, Springer–Verlag, New York, 1981.

[9]Pobst, J. A., Wysong, I. J., and Spores, R. A., "Laser Induced Fluorescence of Ground State Hydrogen Atoms at Nozzle Exit of an Arcjet Thruster," AIAA Paper 95-1973, June 1995.

[10]Liebeskind, J. G., Hanson, R. K., and Cappelli, M. A., "Flow Diagnostics of an Arcjet Using Laser-Induced Fluorescence," AIAA Paper 92-3243, July 1993.

[11]Ruyten, W. M., and Keefer, D., "Two-Beam Multiplexed Laser-Induced Florescence Measurements of an Argon Arcjet Plume," *AIAA Journal*, Vol. 31, No. 11, 1993, pp. 2083–2089.

[12]Rhodes, R. P., and Keefer, D., "Numerical Modeling of an Arcjet Thruster," AIAA Paper 90-2614, July 1990.

[13]Rhodes, R., and Keefer, D., 'Comparison of Model Calculations with Experimental Data from Hydrogen Arcjets," 22nd International Electric Propulsion Conf., Viareggio, Italy, Oct. 1991 (Paper 91-111).

[14]Rhodes, R., and Keefer, D., "Modeling Arcjet Space Thrusters," AIAA Paper 91-1994, June 1991.

[15]Keefer, D., Moeller, T., Rhodes, R., and Ruyten, W., "Multiplexed Laser Induced Fluorescence and Non-Equilibrium Processes in Arcjets," AIAA Paper 94-2656, June 1994.

[16]Zollweg, R. J., and Liebermann, R. W., "Electrical Conductivity of Nonideal Plasmas," *Journal of Applied Physics*, Vol. 62, No. 9, 1987, pp. 3621–3627.

[17]Haag, T. W., "Thrust Stand for High-Power Electric Propulsion Devices," *Review of Scientific Instruments*, Vol. 62, No. 5, 1991, pp. 1186–1191.

[18]Haag, T. W., and Curran, F. M., "Arcjet Starting Reliability: A Multistart Test on Hydrogen/Nitrogen Mixtures," AIAA Paper 87-1061, May 1987.

[19]Ruyten, W. M., Burtner, D., and Keefer, D., "Laser-Induced Fluorescence Measurements on the Plume of a 1 kW Arcjet Operated on Simulated Ammonia," 23rd International Electric Propulsion Conf., Seattle, WA, Sept. 1993.

[20]Ruyten, W. M., and Keefer, D., "Absolute Doppler Shift Calibration of Laser Induced Fluorescence Signals Using Optogalvanic Measurements in a Hollow Cathode Lamp," *Applied Physics Letters*, Vol. 61, No. 8, 1992, pp. 880–882.

[21]Welle, R. P., Pollard, J. E., Janson, S. W., Crofton, M. W., and Cohen, R. B., "One Kilowatt Hydrogen and Helium Arcjet Performance," 27th Joint Propulsion Conf., Aerospace Rept. ATR-91(8343)-2, Sacramento, CA, June 1991.

[22]Welle, R. P., Pollard, J. E., Janson, S. W., Crofton, M. W., and Cohen, R. B., "One Kilowatt Hydrogen and Helium Arcjet Performance," 27th Joint Propulsion Conf., Aerospace Rept. ATR-91(8343)-2, Sacramento, CA, June 1991.

[23]Capelli, M. A., "Fundamental Studies of the Electrode Regions in Arcjet Thrusters," U.S. Air Force Office of Scientific Research Contractors Meeting, Chicago, IL, May 1995.